



Antibacterial and Antifungal Efficacy of Silver Nanoparticles Biosynthesized Using Leaf Extract of *Thymus algeriensis*

Mohammed Beldjilali¹ · Khaled Mekhissi¹ · Yasmina Khane^{1,2} · Wahiba Chaibi³ · Lahcène Belarbi¹ · Smain Bousalem¹

Received: 3 September 2019 / Accepted: 18 October 2019 / Published online: 25 October 2019
© Springer Science+Business Media, LLC, part of Springer Nature 2019

Abstract

The present study reports a cost effective and environment friendly technique for the preparation of silver nanoparticles (AgNPs) using *Thymus algeriensis leaf extract* as reducing and capping agent. The effects of reactants ratio, contact time, pH and temperature on the synthesis of the Ag nanoparticles were investigated. It was found that the rate of formation of silver nanoparticles enhanced with time at high temperature and alkaline pH. The biogenic AgNPs were characterized by UV–Visible spectrophotometer, showing a typical surface Plasmon resonance at about 430 nm which is specific to AgNPs. XRD and SEM–EDX results reveal that the synthesized nanoparticles have a face centered cubic structure (fcc). TEM images clearly show that the biosynthesized nanoparticles are mostly spherical with an average particle sizes between 10 and 20 nm. Fourier transform infrared spectroscopy (FTIR) was used to identify the biomolecules and capping reagents in the *T. algeriensis* leaf extract that may be responsible for the reduction of silver ions and the stability of the bio-reduced nanoparticles. The AgNPs as potential anti-bacterial and anti-fungal agents have been studied on gram negative (*P. aeruginos* and *E. coli*), gram positive (*B. cereus*, and *S. aureus*) pathogenic clinical bacteria and pathogenic fungi (*Candida albicans*). The results showed that the biologically synthesized AgNPs exhibit interesting anti-bacterial and anti-fungal activity with those clinical pathogens.

Keywords Silver nanoparticles · *Thymus algeriensis* · Anti-bacterial · Anti-fungal

1 Introduction

The noble metal nanoparticles, namely silver (Ag), gold (Au) and platinum (Pt) have received a great deal of attention due to their interesting and unique properties that allow attractive applications in various fields such as medicine, cosmetics, biotechnology, biomedical devices and environmental remediation [1]. The large fraction of surface atoms and high surface area of metal nanoparticles are responsible for their unusual properties such as catalytic, electronic and optical absorption [2]. Among several Noble metals, silver nanoparticles have gained more attention in the areas

of nanotechnology and nanomedicine within the last decade due to their excellent catalytic, optical, electrical and antifungal/antibacterial applications [3, 4]. Several techniques have demonstrated that AgNPs can be synthesized using chemical and physical methods [5], but some of them suffer from their lengthy procedure, time consuming, short stability and adsorption of toxic chemicals that might lead to adverse effects in medical applications [6]. Consequently, there is a need to develop an expedient method that can provide free stable nanoparticles with low toxicity. To achieve this goal, many researchers have diverted their interest to the green chemistry approaches for synthesis of silver nanoparticles by using microorganisms, enzyme or plant extract [7, 8]. The green synthesis of Ag NPs has been recently reported, where plant extracts such as *S. tricobatum*, *S. cumini*, *C. asiatica*, *C. sinensis* [9], *Callicarpa maingayi* [10], *Momordica charantia* [11], tea [12], *neem* [13] *ulva intestinalis* extract [14] are effective extracts in the biosynthesis of Ag NPs.

Using plant extracts in the green synthesis of nanoparticles is one of the cleanest, biocompatible, nontoxic and eco-friendly methods. It has many advantages such as easily

✉ Mohammed Beldjilali
chimie005@outlook.fr

¹ Laboratory of Applied Chemistry (LAC), University Center Belhadj Bouchaib, Ain Témouchent, Algeria

² University of Ghardaia, BP 455, Ghardai, Algeria

³ Scientific and Technical Research Center in Chemistry and Physics Analysis (CRAPC), 42415 Bousmail, Tipaza, Algeria

available, safe to handle and possess a broad viability of phytochemicals such as phenolic compounds, flavonoids, terpenoids, polysaccharides, enzymes and other proteins, which are responsible for reduction of metal ions and stabilization of nanoparticles [15, 16]. *Thymus algeriensis* is a very common traditional medicinal herb abundantly available in Algeria and the extract of the leaf has traditionally been used in respiratory and digestive tube disorders and against abortion [17]. Oxygenated monoterpenes, linalool, thymol and p-cymene were the most abundant reported compounds [18].

In this present study we have investigated the synthesis of silver nanoparticles in aqueous medium using aqueous extract of the *T. algeriensis* as reducing as well as stabilizing agent. We have also undertaken the study of antibacterial activity of this as-synthesized AgNPs against two Gram-positive and two Gram negative human bacterial pathogens. The antifungal activity of AgNPs has also been investigated.

2 Experimental

2.1 Materials and Methods

Thymus algeriensis leaf was collected from the Forest area in Tlemcen, northwestern Algeria in April 2013. Silver nitrate (AgNO_3) was supplied by Sigma Aldrich. The clinical isolates of bacterial strains of *Staphylococcus aureus* ATCC 25923, *Pseudomonas aeruginosa* ATCC 27853, *Escherichia coli* ATCC 25922, *Bacillus cereus* ATCC 10876 and *Candida albicans* ATCC 10231 were kindly donated by the Laboratory of Biology of Microbial Systems (LBSM, Ecole Normale Supérieure of Kouba, Algier, Algeria.). Ultra-pure deionized water was used in all the experiments. All the chemicals used were of analytical grade. The glasswares used for experimental purposes were properly washed, sanitized and autoclaved.

2.2 Plants Extract Preparations

Collected fresh leaves were cut into small pieces, and thoroughly washed under running tap water followed by double-distilled water. Aqueous extract of the plant was obtained by soaking 10 g of dried leaves in 200 mL of distilled water and heated at a temperature between 70 and 80 °C for 15 min. It was then allowed to cool and filtered with Whatman Filter Paper No. 1. The filtrate obtained was stored at 4 °C for further experiments.

2.3 Synthesis of Silver Nanoparticles

AgNPs were synthesized by dropwise addition of the aqueous plant extract to the silver nitrate solution of known concentration in an Erlenmeyer flask under stirring for 24 h,

which resulting in a brown color solution indicating the formation of AgNPs. The obtained nanoparticles were subjected to washing (thrice) with double distilled water and analyzed by UV–Vis spectrophotometer. The pH effect on nanoparticle synthesis was determined by maintaining pH with the 1 N NaOH, and 1 N HCl of the reaction mixture to pH 3.0, 5.0, 7.0, 9.0, 11.0, and 13. To determine the effect of temperature and reaction incubation time on AgNPs synthesis, reactions were performed at different temperatures (12, 30 and, 60 °C) and different time intervals (10–360 min) respectively. The impact of silver nitrate concentration on the synthesis of AgNPs was also determined by using different concentration of AgNO_3 (1–5 mM). The reactions was conducted at 1:9 ratio of plant extract and AgNO_3 solution. Thereafter, absorbance of the AgNPs suspension was obtained using UV–Vis spectrophotometer.

2.4 Characterization of AgNPs

Surface plasmon resonance (SPR) of AgNPs was monitored using UV–Vis spectrophotometer (Halo DB-20 Dynamica double beam spectrophotometer) at regular time interval.

The functional groups in the synthesized silver nanoparticles and plant extracts were recorded using Agilent Cary 640 FTIR spectrophotometer in the range of 400–4000 cm^{-1} at a resolution of 4 cm^{-1} at room temperature.

The morphology of the nanoparticles was determined using COXAM scanning electron microscope coupled with EDX (SEM–EDX). The equipment was operated at 25 kV acceleration voltage with a magnification of $\times 30,000$.

The AgNPs were also characterized using Transmission electron microscope (TEM) model Zeiss EM 900 instrument. Prior to TEM analysis, the samples were sonicated for an hour and a drop of the AgNPs solution placed on carbon coated copper grids, dried by evaporation and analyzed at an accelerating voltage of 80 kV.

XRD analysis was recorded by Philips (PW 1710) Diffractometer using $\text{CuK}\alpha$ radiation ($\lambda = 1.5406 \text{ \AA}$), with a 2 θ range from 2 $\theta = 10^\circ$ –80°. To identify the structure and the crystallinity of the silver nanoparticles.

To appraisal the particle size distribution and zeta potential of silver nanoparticles was calculate using Zetasizer Nano Instrument (Malvern) and the analysis were taken at 25 °C with 90° angle.

2.5 Antibacterial and Antifungal Study

The antibacterial activities of AgNPs was investigated by standard agar-well diffusion method against gram negative (*P. aeruginosa* and *E. coli*) and gram positive (*B. cereus*, and *S. aureus*) pathogenic clinical bacteria and pathogenic fungi (*Candida albicans*). Afterward, 100 μL of the suspension containing 100 CFU mL^{-1} of the test

microorganisms were swabbed uniformly on nutrient agar. Two circular wells, for 6 mm diameter were made using a sterile cork-borer. The first well was loaded with a leaf extract as a negative control and the other well was loaded with 40 μL AgNPs ($20 \mu\text{g mL}^{-1}$). The inoculated plates were incubated at 37 °C overnight in an incubator for 24 h. The measurement of the diameter of inhibition zone indicates the inhibitory action of the samples on the growth of the bacteria.

3 Results and Discussion

3.1 FTIR Characterization of *T. algeriensis*

FTIR spectrum of *T. algeriensis* leaf extract (Fig. 1) shows very broad band centred at 3350 cm^{-1} corresponds to OH stretching vibrations of phenol/carboxylic group present in extract [19]. The medium bands at 1404 cm^{-1} and 1568 cm^{-1} corresponds to amide arising due to carbonyl stretch in proteins. The strong peak at 1105 cm^{-1} corresponds to C–N stretching vibration of the amine (Fig. 2).

3.2 UV–Vis Characteristics

The elaboration of silver nanoparticles by the leaf extract of thymus was monitored by UV–Visible spectra. The transformation of silver nitrate into silver nanoparticles was noticed by the change in the color of the solution. The aqueous solution changes from yellow to brown due to the optical properties of silver nanoparticles. This phenomenon is called surface Plasmon resonance (SPR). The peak of silver nanoparticles is sensitive with high absorbance in wavelength at 430 nm and that's confirmed the formation of AgNPs [20].

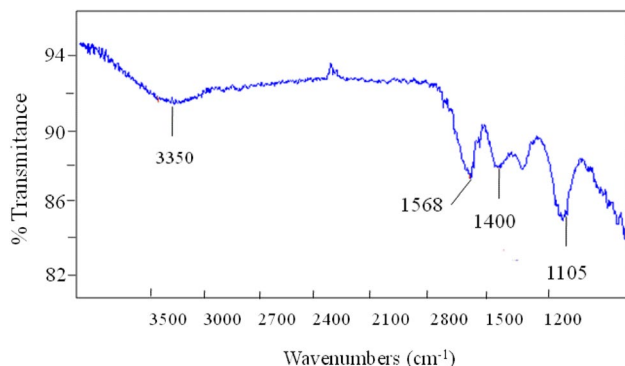


Fig. 1 FTIR spectra representing the functional groups of *T. algeriensis* leaf extract

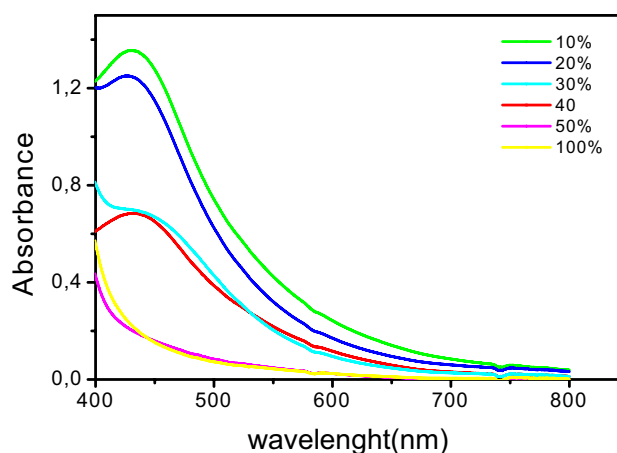


Fig. 2 UV–Vis spectra of AgNPs at different ratio of leaf extract

3.2.1 Effect of Ratio of Plant Extracts and Silver Nitrate Solution

The reaction was performed by varying dosage of *T. algeriensis* leaves extract (v/v) from 10 to 50% keeping other parameters constant at 60 min of exposure time and 1 mM AgNO_3 concentration. It was found that at 10% inoculum dose a consistent increase in the intensity of the surface plasmon peak absorbance for AgNPs was found in UV–Vis spectrum. Thereafter the band intensity decreased with increase in *T. algeriensis* from 20 to 50% [21].

3.2.2 Effect of pH

The pH of the solution is an important parameter which affects the formation of nanoparticles. The change in pH affects the shape and size of the particles, as pH has the ability to change the electrical charges of biomolecules, which might affect their capping and stabilizing abilities and subsequently the growth of the nanoparticles.

Figure 3 shows change in peak absorption wavelength and intensity on varying the pH of the solution. As the pH increases from 3 to 11, the colorless AgNO_3 solution changed to reddish-brown (pH 9) and dark brown (pH 11) after 1 h of reaction. It must be remarked that the absorption peak shifted towards lower wavelength (from 425 nm to 418 nm) indicating a decrease in the size of synthesized AgNPs [22]. However, there was no color change observed for AgNO_3 solutions at a lower pH (pH 3 and 5). In addition to the spectral shift, the absorption intensity increases with increasing pH. This indicated that the alkaline pH environment enhanced the reducing and stabilizing capability of the antioxidants in the *T. algeriensis* leaf extract.

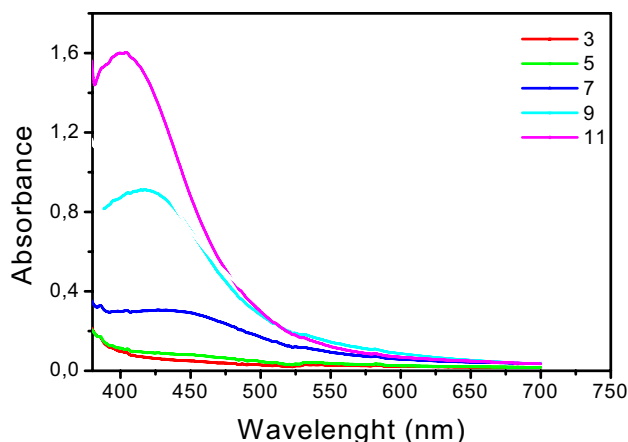


Fig. 3 UV-Vis spectra of AgNPs at different pH

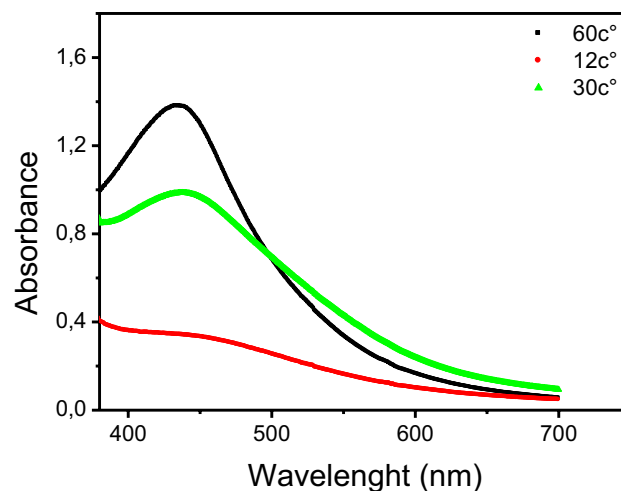


Fig. 5 UV-Vis spectra of AgNPs as function of temperature

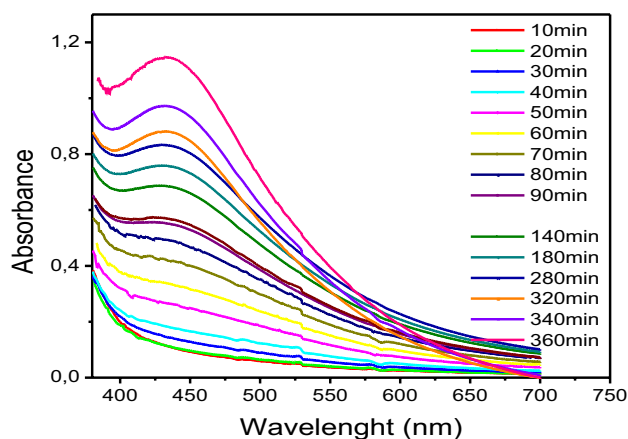


Fig. 4 UV-Vis spectra of AgNPs as different function of time at room temperature

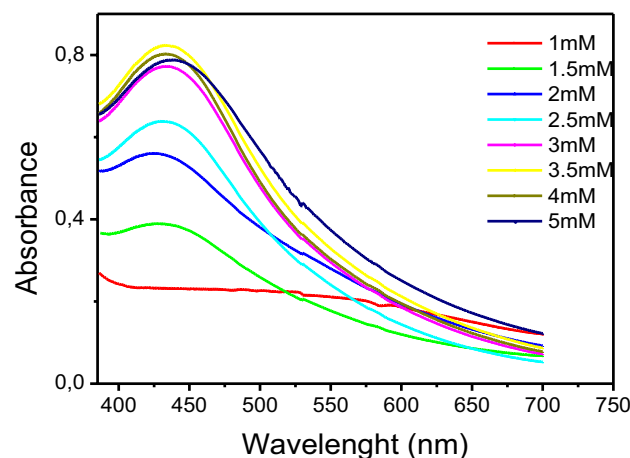


Fig. 6 UV-Vis spectra of AgNPs at different concentration of AgNO₃

3.2.3 Effect of Contact Time

Figure 4 shows the UV-Visible spectra of Ag nanoparticles as function of time after addition of 1 mL *T. algeriensis* leaf extract to 9 mL of 10^{-3} M AgNO₃ solution. The synthesis of AgNPs was observed after 40 min. The solution turned from light yellow to brown in color indicating reduction of silver ions. It was also noted that with an increase in time the peak becomes sharper and intense. The increase in intensity could be due to increasing number of nanoparticles formed as a result of reduction of silver ions presented in the aqueous solution. The reaction was performed till 360 min and the AgNPs showed characteristic peak around 430 nm.

3.2.4 Effect of Temperature

To determine the effect of reaction temperature, the reactions were run at different temperatures (12, 30 and 60 °C).

Figure 5 shows the progress of Ag NPs formation monitored by UV-Vis spectroscopy. A time-dependent relationship of Ag NPs concentration is observed, as the absorption intensity steadily increases while time elapses. Furthermore, a slightly blue shift occurred from 425 to 418 nm at higher temperature (60 °C) indicating a larger amount of small particle size AgNPs was formed.

3.2.5 Effect Concentration of Silver Nitrate

Figure 6 shows the UV-Visible spectra of AgNPs at different AgNO₃ concentration. Increasing AgNO₃ concentration resulted in gradual increasing of absorbance peak between 417 and 437 nm for (1, 2, 3, 4 and 5) mM AgNO₃ which are the characteristic of Ag nanoparticle, due to its surface plasmon resonance absorption band. Interestingly, as the concentration of the AgNO₃ increases, a red shift of the plasmon

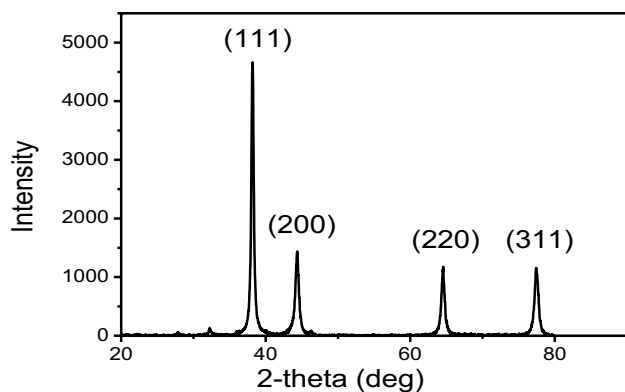


Fig. 7 XRD pattern of AgNps synthesized using *T. algeriensis* leaf extract

resonance bands occurred from 417 at 1 mM to 437 nm at 5 mM, indicating that AgNPs grew larger.

3.3 X-ray Powder Diffraction

To further confirm the formation of nanoparticles, XRD patterns were also recorded in the range of 30° – 70° at 2θ angles for the monometallic Ag. Figure 7 showed the XRD pattern

of AgNPs synthesized by the reaction of aqueous silver salt with *T. algeriensis* leaf extract. The high-intensity peaks of AgNPs were observed at around 38° , 44° , 64° and 77.34° corresponding to (111), (200), (211) and (311) Bragg's reflections of the face-centered cubic crystalline structure of metallic nanoparticles, respectively. Similar results were reported previously for silver nanoparticles [23, 24].

3.4 Scanning Electron Microscopy (SEM)

Figure 8 showing SEM image of silver nanoparticle. The SEM technique was used to calculate the topography and morphology of silver nanoparticles. AgNPs has spherical size with the average (10–20 nm) that were showed by TEM.

3.5 Transmission Electron Microscopy and Energy Dispersive X-ray Analysis

The suitability of the *T. algeriensis* extract in the synthesis of Ag-NPs was proved by direct observation of TEM. Figure 9 shows the transmission electron microscopy characterization of a sample solution of Ag-NPs synthesized by *T. algeriensis* leaf extract. From Fig. 9 it could be seen that the nanoparticles had a spherical shape and the average size of

Fig. 8 SEM analysis of biosynthesized Ag Nps

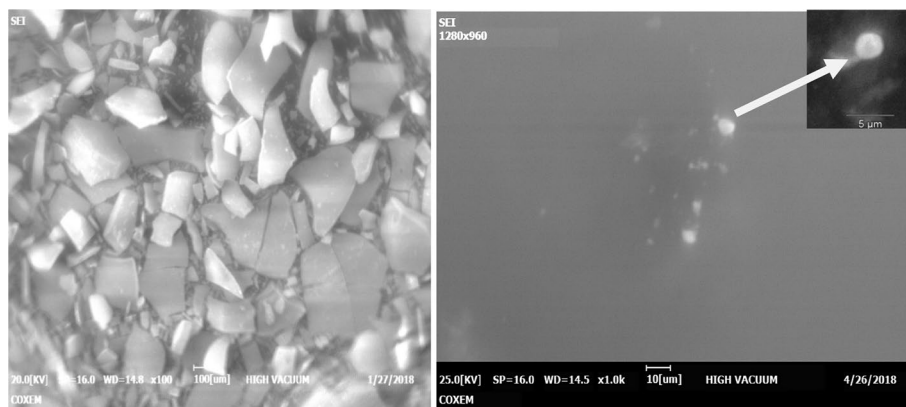
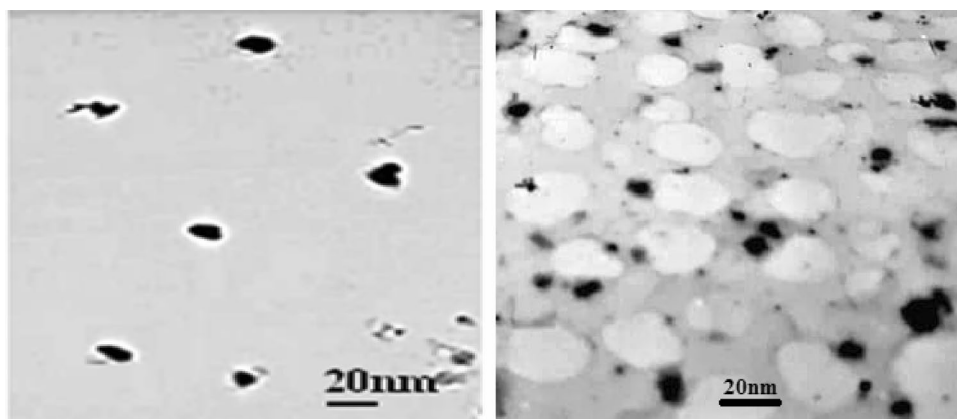


Fig. 9 TEM micrograph of silver nanoparticles



nanoparticles was around 14–20 nm in size, which was in a relatively good agreement with the crystallite size of XRD patterns. The EDX analysis was employed to determine the composition of silver nanoparticles. As shown in Fig. 10, only a strong signal of Ag peak was observed approximately at 3 keV. No other elements could be detected, indicating the high purity of as-obtained AgNPs. This result was in good agreement with XRD analysis.

3.6 Dynamic Light Scatterings (DLS)

The DLS technique was used to determine the hydrodynamic size distribution of the particles. In this process, the size is measured by illuminating the particles in Brownian motion by laser beam. The scattered light from the particles is then analysed by the auto-correlator. The mean particle hydrodynamic size of the AgNPs was found to be 100 nm which

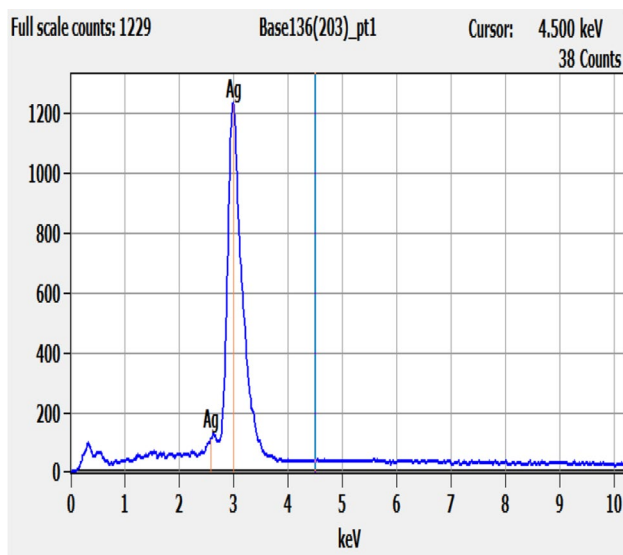
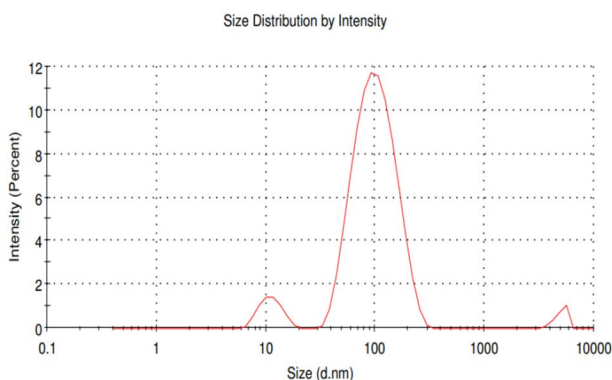


Fig. 10 EDX image of biosynthesized silver nanoparticles using *T. algeriensis* leaf extract



is larger than that observed under TEM. The Zeta potential of -10 mV (Fig. 11), shows that the AgNPs are capped by negatively charged groups, and were dispersed in the medium and proving that they are stable.

3.7 Antimicrobial Activity

During the study, the prepared AgNPs have shown significant antibacterial activity against both Gram-negative and Gram-positive bacteria. The strong inhibitory action was noted against *S. aureus* and *E. coli* with maximum zone of inhibition of 18 and 16 mm respectively, least zone of inhibition was shown around 12 mm for *P. aeruginosa* and 15 mm *B. cereus*. These results agree with those presented by researchers which have reported that *E. coli* (gram negative bacteria) is less susceptible to the silver nanoparticles compared with *S. aureus* (gram positive bacteria [25–27]. however, Kim et al. showed that *S. aureus* was less affected by AgNps compared with *E. coli* even in high concentrations. This could be due to the characteristics of certain bacterial species [28]. Several studies propose the mechanism(s) of the bactericidal action of AgNps. Shrivastava et al. [29] suggested that AgNps may anchor or penetrate the bacterial cell and subsequently modulate cellular signal by dephosphorylating putative key peptide substrates on tyrosine residues (Figs. 12, 13).

In this present test the fungi *Candida albicans* ATCC 10231 show sensitivity against silver nanoparticles synthesized. Its displayed strong antifungal activity with highest zone of inhibition (> 20 mm).

Table 1 shows the result of antibacterial and antifungal activity for biosynthesized AgNPs and aqueous extract of *T. algeriensis*. Clear zone around the disc was considered as the inhibitory effect. It should be pointed out that the negative control (*T. algeriensis* leaf extract) showed no activity towards any of the organisms. Present study findings are in agreement with previous studies against different bacterial strains [30].

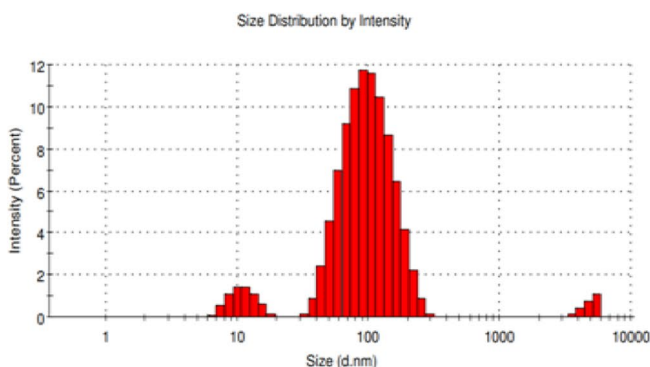


Fig. 11 DLS of silver nanoparticles synthesized using *T. algeriensis* leaf extract

Fig. 12 Zeta potential of silver nanoparticles synthesized using *T. algeriensis* leaf extract

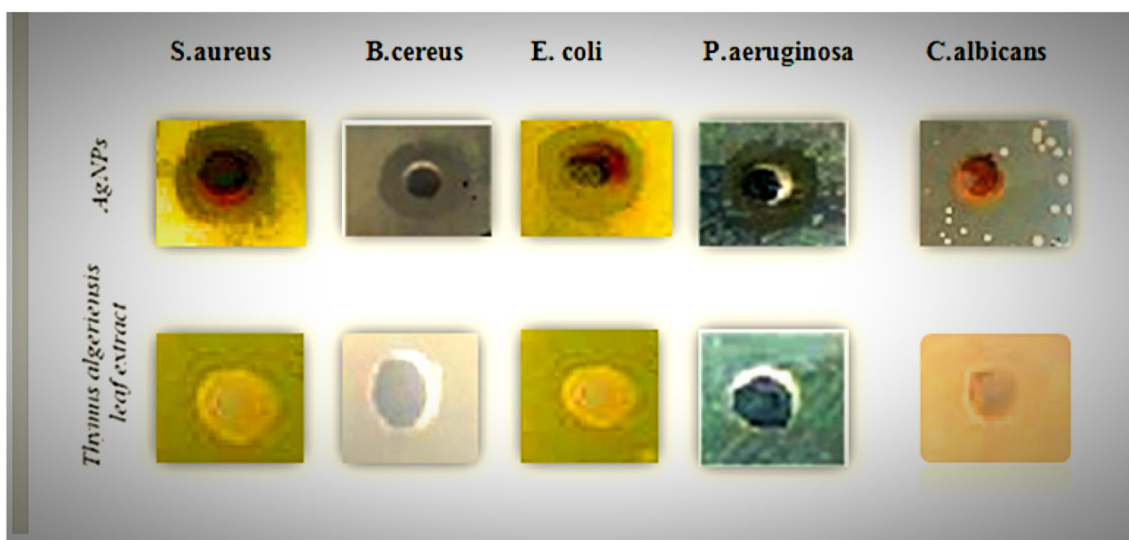
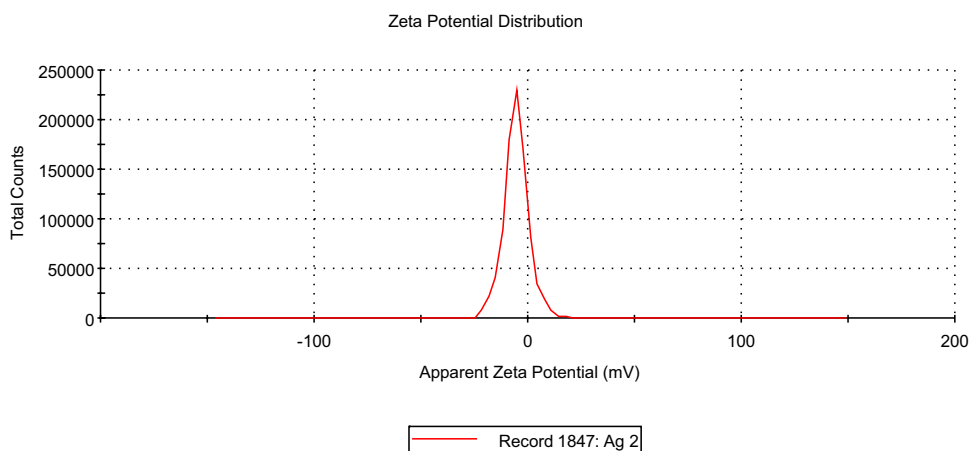


Fig. 13 Antimicrobial activity determined by disc diffusion technique against pathogenic bacteria and fungi

Table 1 The result of antimicrobial activity for biosynthesized AgNPs

| Sample | Pathogenic bacteria | | | | Fungi |
|-----------------------|--------------------------------|--------------------------------|------------------------------------|------------------------------|----------------------------------|
| | Gram + | | Gram – | | |
| | <i>S. aureus</i> ATCC 25923 | <i>B. cereus</i> ATCC 10876 | <i>P. aeruginosa</i> ATCC 27853 | <i>E. Coli</i> ATCC 25922 | <i>C. albicans</i> ATCC 10231 |
| Ag Nps | 18 mm | 15 mm | 12 mm | 16 mm | > 20 mm |
| Leaf extract of plant | No activity | No activity | No activity | No activity | No activity |

4 Conclusions

In conclusion, we have developed, for the first time, an eco-friendly and convenient green protocol for the synthesis of silver nanoparticles via in situ reduction of AgNO_3 in *T. algeriensis* leaf extract as capping and reducing agents. Synthesis conditions were optimized and resultant

nanopowder was characterized using UV–Visible spectroscopy, TEM, DLS and XRD. UV–Vis peak was observed for AgNPs at 430 nm. The crystalline nature of AgNPs was evidenced through XRD and found to be face-centered cubic in nature with spherical shape. A zeta potential result was recorded at -10 mV, which indicates stability of synthesized Ag NPs without addition of any capping agent. Functional groups of plant extract were confirmed

by FTIR. The synthesised AgNPs showed good antifungal and antibacterial activities against both Gram positive and Gram negative pathogenic bacteria. Finally, the green synthesis of silver nanoparticles using plant extract was found to be safe, eco-friendly and it could be a suitable for biomedical applications.

References

1. S. Iravani, *Green Chem.* **13**, 2638–2650 (2011)
2. M.H. Khalil Mostafa, H. Ismail Eman, Z. El-Baghdady Khaled, M. Doaa, *Arab. J. Chem.* **7**(6), 1131–1139 (2014)
3. A. Manikandan, M. Sathiyabama, *J Nanomed Nanotechnol.* **5**, 251 (2015)
4. N. Sharma, K. Phutela, A. Goel, S. Soni, N. Batra, *Biointerface Res. Appl. Chem.* **8**(1), 3100–3104 (2018)
5. K.M. El-Nour, A.A. Eftaiha, A. Al-Warthan, R.A. Ammar, *Arab. J. Chem.* **3**, 135–140 (2010)
6. M. Raffi, A.K. Rumaiz, M.M. Hasan, S.I. Shah, *J. Mater. Res.* **22**, 3378–3384 (2007)
7. C.M. Marquez-Herrera, *Appl. Surf. Sci.* **355**, 341–349 (2015)
8. S. Mohammad, Md.H. Rahman et al., *Nanosci. Nanometrol.* **3**(1), 34–39 (2017)
9. P. Logeswari, S. Silambarasan, J. Abraham, *Sci. Iran.* **20**(3), 1049–1054 (2013)
10. K. Shamel, M. Bin Ahmad, E.A. Jaffar Al-Mulla, N.A. Ibrahim et al., *Molecules* **17**, 8506–8517 (2012)
11. S.A. David, K.M. Ponvel, M.A. Fathima, S. Anita, J. Ashli, A. Athilakshmi, *J. Nat. Prod. Plant Resour.* **4**(6), 1–8 (2014)
12. J.J. Mohindru, UK Garg, *Int. J. Eng. Sci. Res. Technol.* **6**(7), 307–311 (2017)
13. A.J. Gavhane, P. Padmanabhan, S.P. Kamble, *SN Jangle. Int. J. Pharma Bio Sci.* **3**(3), 88–100 (2012)
14. N. González-Ballesteros, L. Diego-González, M. Lastra-Valdor, M.C. Rodríguez-Arguelles, M. Grimaldi, A. Cavazza, F. Bigi, R. Simón-Vázquez, *J. Mater. Chem. B.* **7**, 4677–4691 (2019)
15. K. Selvam, C. Sudhakar, M. Govarthan et al., *J. Radiat. Res Appl. Sci.* **10**(1), 6–12 (2017)
16. V.L. Das, R. Thomas, R.T. Varghese, E.V. Soniya, J. Mathew, E.K. Radhakrishnan, *3 Biotech* **4**(2), 121–126 (2014)
17. A.A. Giweli, A.M. Džamic, M.D. Sokovic, M.S. Ristić, P.D. Marin, *Cent. Eur. J. Bot.* 504–511 (2013)
18. T. Dob, D. Dahmane, T. Benabdelkader, C. Chelghoum, *Int. J. Aromather.* **16**(2), 95–100 (2006)
19. A. Allafchian, S.Z. Mirahmadi-Zare, S.A.H. Jalali, S.S. Hashemi, M.R. Vahabi, *J. Nanostruct. Chem.* **6**(2), 129–135 (2016)
20. S. Raja, V. Ramesh, V. Thivaharan, *Arab. J. Chem.* **10**(2), 253–261 (2017)
21. S. Jain, M.S. Mehata, *Sci. Rep.* **7**(1), 15867 (2017)
22. J.P. Dubey, *Toxoplasmosis of Animals and Man* (CRC Press, Boca Raton, 2010), pp. 1–220
23. R.R. Kannan, W.A. Stirk, J. Van Staden, *S. Afr. J. Bot.* **86**, 1–4 (2013)
24. F. Benakashani, A.R. Allafchian, S.A.H. Jalali, *Karbala Int. J. Mod. Sci.* **2**, 251–258 (2016)
25. M.M.H. Khalil, E.H. Ismail, K.Z. El-Baghdady, D. Mohamed, *Arab. J. Chem.* **7**, 1131–1139 (2014)
26. I. Sondi, S. Sondi, *J. Colloid Interface Sci.* **275**, 177–182 (2004)
27. M. Ghaedi, M. Yousefinejad, M. Safarpour, H.Z. Khafri, M.K. Purkait, *J. Ind. Eng. Chem.* **31**, 167–172 (2015)
28. J.S. Kim, E. Kuk, K.N. Yu, J.H. Kim, S.J. Park, H.J. Lee, S.H. Kim, Y.K. Park, Y.H. Park, C.Y. Hwang, Y.K. Kim, Y.S. Lee, D.H. Jeong, M.H. Cho, *Nanomedicine* **3**(1), 95–101 (2007)
29. S. Shrivastava, T. Bera, A. Roy, G. Singh, P. Ramachandrarao, D. Dash, *Nanotechnology* **18**, 225103 (2007)
30. M.P. Patil, A.A. Rokade, D. Ngabire, G.-D. Kim, *J. Clust. Sci.* **27**, 1737–1750 (2016)

Publisher's Note Springer Nature remains neutral with regard to jurisdictional claims in published maps and institutional affiliations.